Theor Chem Acc (2006) 116: 480–485
DOI 10.1007/s00214-006-0084-6

REGULAR ARTICLE

Javier Fernández Sanz · Antonio M. Márquez

Structure and dynamics of methyl-substituted beryllocene: $[Be(C_5Me_5)_2]$

Received: 18 November 2004 / Accepted: 5 March 2005 / Published online: 21 February 2006

Abstract In this paper we study theoretically the molecular structure of $[Be(C_5Me_5)_2]$, with special interest in similarities and differences found in the computed geometric parameters, depending on the treatment of the electron correlation used. Given the low energy differences found between the different configurations studied (less than 4 kcal mol^{-1}), and the high fluxionality found in experimental studies for this compound, we analyzed the dynamics of the system by means of first principles molecular dynamics calculations. A complex dynamics is found and analyzed in terms of two molecular rearrangement processes: 1,2-sigmatropic intra-ring rearrangement and a ring inversion mechanism that interchanges the roles (with regard to their coordination to the central Be atom) of the two rings.

Keywords Beryllium · Cyclopentadienyl ligands · Electronic structure · Molecular dynamics · Metallocenes · Half-sandwich complexes

1 Introduction

The molecular structure and dynamics of beryllocene ($BeCp_2$, Cp=C_5H_5 (**1**)), the lightest member of the general bis-metallocene series of compounds $[MCp'_2]$, have been the subject of intensive studies since its discovery in 1959. In 1972, Wong et al. [1] reported the first low-temperature X-ray crystal structure analysis of **1**. The two Cp rings were found to be parallel but staggered to each other in what is known as a 'slip-sandwich' structure with the Be atom showing a η^5-coordination mode towards one of the Cp rings and η^1- to the other (see Fig. 1). This asymmetric geometry is in contrast to the well-known η^5/η^5 structure of ferrocene, for instance.

Theoretical calculations of different types and computational complexity have been done over the years (see, e.g., [2,3] and references therein) to understand the structure of **1**, although results have not been conclusive. The dynamic behavior of **1** has been analyzed by Magrl et al. [4,5] using Car-Parrinello molecular dynamics (MD) calculations. The simulation leads to an interpretation of the dynamics of this compound in terms of two processes: 1,2-sigmatropic rearrangement on the η^1- ring and intramolecular exchange by inversion of the coordination modes of the η^1- and η^5- rings.

Recently, Conejo et al. [6,7] have prepared a number of substituted beryllocenes, including $BeCp^*_2$ ($Cp^* = C_5Me_5$, **2**), $Be(C_5Me_4H)_2$ (**3**) and $Be(Cp^*)(C_5Me_4H)$ (**4**). The molecular structure of **2** from X-ray diffraction data revealed that, unexpectedly for this compound, the η^5/η^5 structure is favored in the solid state. This was taken as an indication of the existence of an equilibrium between the formation of a localized Be–C σ bond and a delocalized interaction with the ring π-system that, depending on the balance of forces, favors either the 'slip-sandwich' or the more regular η^5/η^5 structure. Theoretical calculations and bonding analysis on (**1**–**4**) molecular systems [7] performed at different levels of theory showed that the balance of forces is extremely delicate in these systems. Conejo et al. have also provided experimental evidence [6] for the presence of the η^5, η^1-isomer of **2** in solution, and of the molecular rearrangement of the η^5- and η^1- rings.

More recently, Hung et al. [8], have studied the correlation between anisotropic ^{9}Be NMR interactions and the structure and dynamics in **1**–**3**, by using solid-state ^{9}Be NMR spectroscopy and variable temperature ^{9}Be and ^{13}C NMR experiments. Their results reveal a highly fluxional structure in the condensed phase for **1**, motion averaging of the NMR parameters in **2** due to molecular motions at higher temperatures and no temperature dependence of the ^{9}Be NMR spectra for **3**. Experiments at temperatures $\sim$ 173 K, however, support the idea of decelerating Cp* ring motions in **2** at these low temperatures. All these results indicate a highly

Dedicated to Dr. Jeal Paul Malrieu on occasion of his 65th birthday.

Javier Fernández Sanz · Antonio M. Márquez (✉)
Departamento de Química Física, Universidad de Sevilla,
Facultad de Química, CL/Prof. García González s/n,
41012 Sevilla, Spain
E-mail: sanz@us.es, marquez@us.es
Tel.: 34-954557177
Fax: 34-954557174

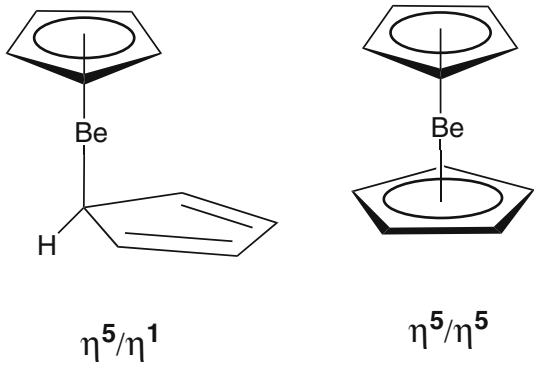

Fig. 1 Slip-sandwich and parallel structures of beryllocenes

fluxional structure on these systems with rapid reorientation of the rings and possible exchange of the rings.

In this paper, we study theoretically the molecular structure of $BeCp_2^*$, with special interest in the similarities and differences found in the computed geometric parameters depending on the treatment of the electron correlation used. Given the low energy differences found between the different configurations studied, and the high fluxionality found in experimental studies for this compound, we analyzed the dynamics of the system by means of first principles MD calculations. The MD data analysis is focused mainly on two processes: the 1,2-sigmatropic intra-ring rearrangement, and the interring conversion mechanism. A comparison with the dynamics of $BeCp_2$ is also made.

2 Computational details

2.1 Structure

In all cases, except where explicitly indicated, we have employed the 6-31G(d, p) atomic basis set for all elements. This basis set, of double-ζ quality and including polarization orbitals on all atoms, is known to give a quite reasonable description of the atomic electron density. Restricted Hartree-Fock (RHF) and density functional theory (DFT) calculations have been performed using the Gaussian 98 suite of programs [9]. Various functionals have been employed, combining Becke's three-parameter hybrid exchange functional [10], with either the non-local correlation functional of Lee et al. [11] (B3LYP) or the non-local correlation functional of Perdew [12] (B3PW91) and the gradient-corrected exchange functional of Perdew [13] with the same non-local correlation functional of Perdew (PW91). CASSCF calculations have also been undertaken to check for possible effects of the non-dynamical correlation in the electronic structure of the complexes studied here. The valence structure of the $BeCp'_2$ systems is complex, due to the large number of electrons presents. To adequately describe the bonding between the Be atom and the two Cp' rings, the logical choice for the active space will include the valence shell of the Be atom and the π-system of both Cp' rings. This produces an active space consisting of 12 electrons distributed over 14 molecular orbitals. Given that the last MO in this active space was found, in preliminary calculations, to be practically empty, we have deleted it from the active space and, finally, kept an active space of 12 electrons distributed over 13 MOs that produces a CI wavefuction of 736164 CSF. This active space is expected to adequately describe near degeneracy effects of both intra Cp' π-systems and those resulting in charge transfers between the Be atom and Cp' rings. These CASSCF calculations have been undertaken using a locally modified version of the HONDO program system [14] that allows us to perform direct and parallel CI calculations in a Beowulf-type computer.

2.2 First principles MD calculations

The dynamic behavior of substituted beryllocenes was analyzed from first principles MD simulations carried out in the Born-Oppenheimer surface using the VASP 4.6 code [15,16]. The energy was obtained using the generalized gradient correction (GGA) implementation of DFT proposed by Perdew et al. [17]. The ultra-soft pseudopotential (US-PP) approach of Vanderbilt [18] was used to represent the core electrons and the electronic states were spanned using plane waves as basis set with an energy cutoff of 215 eV. To integrate Newton's equations a Verlet algorithm was used with a time step of 2 fs. The system was initially thermalized at 300 K in a run of 5 ps where the velocities were rescaled every ten steps. Further simulations at 350 and 400 K were performed using a Nosé thermostat [19,20].

3 Results and discussion

3.1 Structure

While DFT functionals, widely employed nowadays, give reasonably accurate and consistent results for systems well described with a single Slater determinant, it has been suggested that, in cases with near degeneracy effects present, more than one determinant may be needed to construct the exact energy functional. For these reasons, we have undertaken CASSCF calculations to check for possible effects of quasi-degeneracy effects in the electronic structure of the systems studied here. However, one has to take the CASSCF results with caution as they may give an unbalanced description of the electronic structure of the system. If only part of the valence electrons are included in the active space, all the non-dynamical correlation effects are recovered on the active space but none in the inactive space or between the inactive and the active electrons. The dynamical correlation effects, not explicitly included in the CASSCF wavefunction may also be important in determining the electronic features of the system. For these reasons, we have performed calculations with various DFT functionals, including those that merge part of the HF exchange in the functional, like the B3LYP and B3PW91. The design of our CASSCF calculations tries to give a balanced description of the non-dynamical correlation effects in the bonding between the Cp' ring and

Table 1 Calculated main geometrical parameters (Å and degrees) and relative energies of the C_s isomers (kcal mol^{-1} with respect to the D_{5d} structure)

Molecule/Symmetry	Level	r^a_{BeC}	r^a_{BeX}	r^a_{CC}	$\alpha^b_{XBeC_1}$	$\beta^b_{BeC_1X'}$	E^c_{rel}
$BeCp_2$ /D_{5d}	RHF	2.067	1.685	1.407			
	B3LYP	2.054	1.662	1.419			
	PW91	2.047	1.650	1.424			
	BPW91	2.054	1.658	1.426			
	B3PW91	2.042	1.649	1.417			
	CASSCF	2.085	1.703	1.415			
$BeCp_2$ /C_s	RHF	1.920–1.935	1.511	1.409–1.411	179.2	112.8	−6.27
		1.763–3.365	2.523	1.346–1.480			
	B3LYP	1.908–1.935	1.497	1.420–1.423	176.7	104.4	−2.52
		1.786–3.201	2.389	1.375–1.470			
	PW91	1.901–1.926	1.502	1.425–1.429	172.7	92.0	0.93
		1.777–2.951	2.197	1.395–1.459			
	BPW91	1.908–1.953	1.505	1.427–1.431	172.8	94.8	0.57
		1.778–3.016	2.247	1.393–1.464			
	B3PW91	1.897–1.936	1.493	1.417–1.421	173.9	96.0	0.63
		1.770–3.027	2.259	1.382–1.456			
	CASSCF	1.957–1.966	1.550	1.416–1.417	179.9	113.7	−9.41
		1.783–3.418	2.563	1.359–1.491			
$BeCp^*_2$ /D_{5d}	RHF	2.081	1.698	1.414			
	B3LYP	2.069	1.676	1.427			
	PW91	2.062	1.663	1.433			
	BPW91	2.074	1.677	1.435			
	B3PW91	2.059	1.665	1.425			
	CASSCF	2.087	1.701	1.421			
$BeCp^*_2$ /C_s	RHF	1.916–1.927	1.500	1.417–1.420	179.1	109.0	−8.53
		1.779–3.310	2.487	1.347–1.493			
	B3LYP	1.905–1.925	1.484	1.429–1.433	176.8	102.2	−3.59
		1.773–3.175	2.374	1.378–1.484			
	PW91	1.889–1.936	1.485	1.435–1.439	172.0	92.5	0.04
		1.782–2.975	2.217	1.398–1.473			
	BPW91	1.928–1.938	1.490	1.438–1.442	174.8	98.3	−1.11
		1.788–3.111	2.323	1.393–1.482			
	B3PW91	1.896–1.923	1.478	1.427–1.431	175.0	97.7	−0.70
		1.779–3.078	2.300	1.382–1.472			
	CASSCF	1.963–1.964	1.547	1.422–1.425	165.6	87.7	−3.24
		1.802–2.851	2.144	1.384–1.466			

[a] For the C_s structures the first line of the geometrical parameters r_{BeC}, r_{BeX}, and r_{CC} corresponds to the η^5-ring while the second corresponds to the η^1-ring

[b] X refers to the η^5-ring centroid and X' to the η^1-ring centroid

[c] Relative energies for the C_s isomer taking the corresponding D_{5d} structure as reference

the central Be atom. Thus, we have included all the valence electrons involved, including the valence electrons of Be and the ten electrons of the π systems of the two Cp' rings.

In Table 1, the results on the computed geometries, enforcing either D_{5d} or C_s symmetry, of **1** and **2** at different theory levels are summarized. Although several papers in the recent literature report theoretical studies of the structure of **1**, none of them has made an extensive comparison of electron correlation effects in this or related systems. A limited discussion of the effects of electron correlation on the geometry of these systems has already been presented by the authors in Ref. [7].

The optimized geometries for the D_{5d} structures are similar to each other. Irrespective of the theoretical level used, only small tendencies can be noticed. The DFT functionals produce the shortest distances, with an average value of 2.049 ± 0.005 Å for the Be–C distance in $BeCp_2$ and 2.066 ± 0.006 Å in $BeCp^*_2$. In both cases, the computed distances are longer at the HF level (2.067 and 2.081 Å) and even longer at the CASSCF level (2.085 and 2.087 Å). These results are significant in the sense that they indicate that the effects of the dynamical electron correlation, mostly accounted for in the DFT functionals, increase the strength of the Be–Cp'(η^5) bond, while the non-dynamical correlation effects, included in the CASSCF wavefunction, reduce the strength of this delocalized bond, thus resulting in a longer Be–Cp(η^5) distance. Comparison of the $BeCp_2$ and $BeCp^*_2$ geometries reveals that there is a small increase of the Be–Cp distances due to the introduction of the methyl groups that amounts to about 0.015 Å at DFT or HF levels. These results are not surprising as the bonding mechanism should be similar in both systems but at the same time they are indicative of the non-existence of steric repulsions between the two bulky Cp' rings. The computed geometry for $BeCp^*_2$ is in good

agreement with the experimental findings although the theoretical values are a little longer (by 0.02 Å) than the experimentally determined bond distances. The floppiness of the molecule and the fact that the experimental values correspond to the solid state, where the packing forces may have a significant influence on the geometry, must be considered when comparing these two sets of theoretical parameters.

The geometries and relative energies computed at different theoretical levels for the C_s structures show some general trends and a few significant differences that indicate that the treatment of the electron correlation effects is determinant to correctly understand the electronic structure and bonding in these complex systems. All Be–C distances to the η^5-ring are smaller than in the corresponding D_{5d} structure (by 0.10–0.15 Å in $BeCp_2$ and by 0.13–0.17 Å in $BeCp_2^*$) with small differences between all DFT levels (about 0.015 Å). Correspondingly, the Be-ring centroid distance is smaller by the same amount, indicating a reinforcement of the delocalized Be–Cp(η^5) bond, following a similar mechanism in both systems where steric repulsions due to the -Me substituents can be discarded. With respect to the η^1 ring, all computed Be–C_1 bond distances (see Fig. 1) are similar, with values between 1.76 and 1.78 Å except for $BeCp_2^*$ at CASSCF level, where, reflecting a noticeable difference in structure, this bond distance is computed at 1.80 Å. Between all DFT levels the computed bond distances are similar, an important qualitative difference appears in the coordination mode of the η^1-ring depending on the correlation functional used. For $BeCp_2$, the C_1 has a tetrahedral coordination at RHF, CASSCF or B3LYP levels while the structures predicted by these functionals employing the PW91 correlation functional can be described more as of the slip-sandwich type, with a Be–C_1–X' [X' = (η^1)-ring centroid] angle close to 90°. This reflects a fundamental difference in the treatment of the electron correlation in this functional that is also reflected on the computed relative energies. The B3LYP functional (as the RHF level) predicts the C_s to be the lower energy structure (by 2.5 kcal mol^{-1} in $BeCp_2$ and by 3.6 kcal mol^{-1} in $BeCp_2^*$), however these functionals employing the PW91 correlation functional give much smaller energy differences between the two isomers, about or less than 1 kcal mol^{-1}. This is consistent with the slip-sandwich description of the η^1-ring coordination, producing a fluxional picture of the structure of these systems. The results given by the CASSCF wavefunction are, however, qualitatively different for $BeCp_2$ than for $BeCp_2^*$. For the former, the structure is of the σ-type, close to the HF description, and the energy difference between the two conformations is larger than in any other theoretical level (9.4 kcal mol^{-1}). However, for $BeCp_2^*$ the CASSCF structure is clearly of the slip-sandwich type with an energy difference between the two conformations of only 3.2 kcal mol^{-1}.

3.2 Dynamics

In Fig. 2, we present some results from the MD runs for $BeCp_2^*$ at $T = 350$ K and $T = 400$ K, showing a time span of 8 ps, Be–C distances for each ring and a hapticity index that intends to reflect the coordination of each ring. To define such a hapticity index we have taken as bound to the Be atom, for each configuration and Cp* ring, the C atom with the minimal distance and others whose distance to the Be atom is not 0.4 bohr greater than the minimal Be–C distance. MD runs at $T = 300$ K show no noticeable motion and are not shown for simplicity in the figure. From the results presented, a dynamics more complex than that found for $BeCp_2$ by Magrl et al. [4,5] was found. To start the analysis of the results presented, one can observe that the Be–C distances fluctuate more in the upper ring than in the lower. Thus, while at 350(400) K the Be–C distance for the lower ring fluctuates between 1.058 and 1.540 (1.065 and 1.754) Å, for the upper ring this fluctuation range increases from 1.062 to 2.175 (1.059 and 2.183) Å. This can be interpreted in the sense that exchange of vibrational energy between the rings is difficult since it should be mediated by vibrations of the central Be atoms that, given its low atomic mass, can transport little vibration energy between the two rings. On the other hand, Me-groups can act as a reservoir of vibrational energy on each ring, thus hampering even more the interchange of roles of the two rings. It should be understood that in condensed phases the interaction with the solvent or with nearby molecules should make this energy exchange much easier.

While $BeCp_2$ shows a sharp ring inversion process [4,5], in the sense that ring interchange occurs with very few or no intermediate configurations, our MD data shows that $BeCp_2^*$ ring inversion happens with many intermediate configurations involved. In general, when one ring changes the hapticity from $^1\eta$ to $^5\eta$ or vice versa, a few configurations with intermediate hapticyties can be seen, in some cases with transition time intervals as long as 0.5 ps. The structures show, in many cases, a η^2/η^2 coordination and can be related to an intermediate which shows this coordination found in the isoelectronic system $[BCp_2^*]^+$ by Kown and McKee [21]. The long time windows of existence of these intermediate structures suggest that, like in the latter study, the η^2/η^2 intermediate may be the lowest energy pathway for ring inversion. Another qualitative difference found is that in $BeCp_2$ both theoretical [4,5] and experimental [8] results, indicate that ring inversion is a concerted process; this is when one ring changes hapticity and the other suffers the opposite change. In $BeCp_2^*$ the dynamics is more involved with time intervals where both rings have high hapticity and time intervals where both have a low coordination to the central Be atom. This reflects the higher fluxionality of **2** compared with **1**, in agreement with the experimental results of Hung et al. [8].

A final point of interest to examine in the MD simulations is the number of molecular rearrangement processes, either the intraring 1,2-sigmatropic rearrangement or the molecular ring inversion. Taking into account the number of intraring rearrangements found in our MD data, the frequency for this process can be estimated to lie in the range of 5.6–9.4 ps^{-1} at 350 K and a little higher, 7.7–9.3 ps^{-1} at 400 K. These numbers are about an order of magnitude higher than those obtained by Magrl et al. for the same process in **1**. For

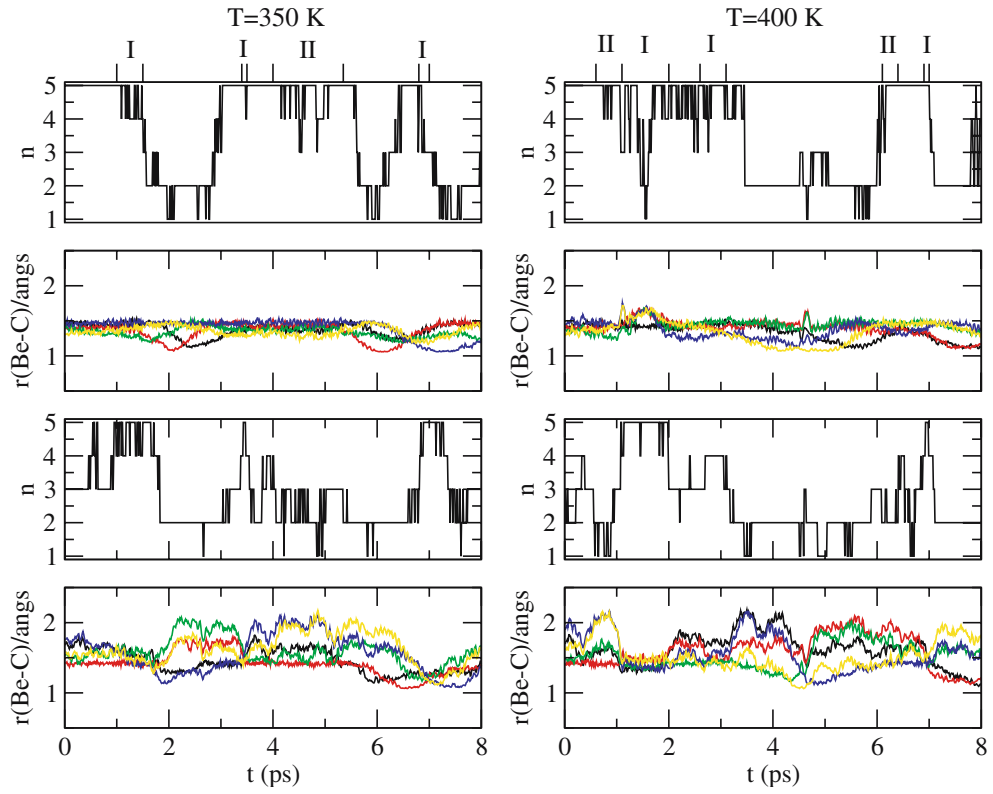

Fig. 2 Time evolution of $BeCp_2^*$ at 350 K (*left*) and 400 K (*right*). The figure shows the trajectories as a plot of the Be-C distances for each ring (r(Be–C) in Å), and a ring hapticity index (n) defined in the text. The intervals indicated in the *upper axis* of the figure represent the time windows dominated by either the D_{5d} structure (I) or the C_s strucure (II). The *upper part* of the diagram correspond to the ring initially having a η^5 coordination and the *lower part* of the diagram to the ring having initially a η^1 coordination (see Fig. 1)

the molecular ring inversion mechanism the frequency can be estimated from our data to be between 0.5 and 1.5 ps^{-1}, given that we can observe between 5 and 13 inversions in the total time span of our MD run. From their MD data on **1**, Magrl et al. [4,5], estimate the same range of frequency for the molecular inversion process. However, these same data show only two ring inversions in a time span of $\sim$ 8 ps and again shows $BeCp_2^*$ as a more fluxional system.

4 Conclusions

The structure and dynamics of $BeCp_2^*$ have been investigated in this paper. By using first principles DFT calculations and extended CASSCF calculations we examine the geometry of the ground state of this system, with special focus on the consequences that the treatment of the electron correlation has on the description of the molecular structure. The computed geometric parameters are in agreement with experimental X-ray data taking into account that the experimental values correspond to the solid state, where the packing forces may have a significant influence on the geometry. Low-energy differences are found between the D_{5d} and C_s structures (less than 4 kcal mol^{-1} at the correlated level of theory), in agreement with experimental reactivity [6] and NMR data [8]. This translates the structural problem to a dynamical problem and thus we have studied by means of MD calculations the dynamical behavior of this system. We find a dynamics more complex in $BeCp_2^*$ than that proposed by Magrl et al. [4,5] for $BeCp_2$: higher fluxionality with larger rates for both 1,2-sigmatropic interring rearrangement and ring exchange processes. For this last process we also found that transition from η^5 to η^1 coordination occurs in long time spans in some cases lasting up to 0.5 ps, and with many intermediate configurations involved.

Acknowledgements Research supported by Spanish DGICYT Grant N. MAT 2002-0576.

References

1. Wong CH, Lee TY, Chao KJ, Le S (1972) Acta Crystallogr Sect B 28:1662
2. Rayón VM, Frenking G (2002) Chem Eur J 8:4693
3. Budzelaar PHM, Engelberts JJ, van Lenthe JH (2003) Organometallics 22:1562
4. Magrl P, Schwarz K, Blöchl PE (1994) J Am Chem Soc 116:11177
5. Magrl P, Schwarz K, Blöchl PE (1995) J Chem Phys 103:683
6. Conejo MM, Fernández R, Carmona E, Andersem RA, Gutiérrez-Puebla E, Monge MA (2003) Chem Eur J 9:4462
7. Conejo MM, Fernández R, del Rio D, Carmona E, Monge MA, Ruiz C, Márquez AM, Fernández Sanz J (2003) Chem Eur J 9:4452

8. Hung I, Macdonald LB, Schurko RW (2004) Chem Eur J 10:5923
9. Frisch MJ, Trucks GW, Schlegel HB, Scuseria GE, Robb MA, Cheeseman JR, Zakrzewski VG, Montgomery JA, Stratmann JRE, Burant JC, Dapprich S, Millam JM, Daniels AD, Kudin KN, Strain MC, Farkas O, Tomasi J, Barone V, Cossi M, Cammi R, Mennucci B, Pomelli C, Adamo C, Clifford S, Ochterski J, Petersson GA, Ayala PY, Morokuma QCK, Malick DK, Rabuck AD, Raghavachari K, Foresman JB, Cioslowski J, Ortiz JV, Baboul AG, Stefanov BB, Liu G, Liashenko A, Piskorz P, Komaromi I, Gomperts R, Martin RL, Fox DJ, Keith T, Al-Laham MA, Peng CY, Nanayakkara A, Gonzalez C, Challacombe M, Gill PMW, Johnson B, Chen W, Wong MW, Andres JL, Head-Gordon M, Replogle ES, Pople JA (1998) Revision A.7 ed., Gaussian Inc: Pittsburgh
10. Becke AD, (1993) J Chem Phys 98:5648
11. Lee C, Yang W, Parr RG, (1988) Phys Rev B 37:785
12. Perdew JP, Wang Y (1992) Phys Rev B 45:13244
13. Perdew JP, Kurth S, Zupan A, Blaha P (1999) Phys Rev Lett 82:2544
14. Dupuis M, Márquez A, Davidson ER, "HONDO 99" (1999) based on HONDO 95.3, Dupuis M, Márquez A, Davidson ER, Quantum Chemistry Program Exchange (QCPE), Indiana University: Bloomington, In 47405
15. Kresse G, Hafner J (1993) Phys Rev B 47:R558
16. Kresse G, Furthmuller J (1996) Comput Mater Sci 6:15; Phys Rev B 54:11169
17. Perdew J, Chevary J, Vosko S, Jackson K, Pederson M, Singh D, Fiolhais C, (1992) Phys Rev B 46:6671
18. Vanderbilt D (1990) Phys Rev B 41:7892
19. Nosé S, (1984) J. Chem. Phys. 81:511
20. Nosé S, (1991) Prog Theor Phys Suppl 103:1
21. Kwon O, McKee KL (2001) J Phys Chem A 105:10133